Dynamic PRA of Flooding-Initiated Accident Scenarios Using THALES2-RAPID

Kotaro Kubo, Xiaoyu Zheng, Yoichi Tanaka, Hitoshi Tamaki and Tomoyuki Sugiyama
Japan Atomic Energy Agency, Japan. E-mail: kubo.kotaro@jaea.go.jp

Sunghyon Jang, Takashi Takata and Akira Yamaguchi
The University of Tokyo, Japan. E-mail: kubo@nse.t.u-tokyo.ac.jp

Probabilistic risk assessment (PRA) is one of the methods used to assess the risks associated with large and complex systems. When the risk of an external event is evaluated using conventional PRA, a particular limitation is the difficulty in considering the timing at which nuclear power plant structures, systems, and components fail. To overcome this limitation, we coupled thermal-hydraulic and external-event simulations using Risk Assessment with Plant Interactive Dynamics (RAPID). Internal flooding was chosen as the representative external event, and a pressurized water reactor plant model was used. Equations based on Bernoulli's theorem were applied to flooding propagation in the turbine building. In the analysis, uncertainties were taken into account, including the flow rate of the flood water source and the failure criteria for the mitigation systems. In terms of recovery action, isolation of the flood water source by the operator and drainage using a pump were modeled based on several assumptions. The results indicate that the isolation action became more effective when combined with drainage.

Keywords: Dynamic PRA, THALES2, RAPID, Flooding PRA, Severe Accident, External Event

1. Introduction

Probabilistic risk assessment (PRA) is one of the methods used to assess the risks associated with large and complex systems. The typical PRA techniques of event trees and fault trees are used to organize the logic that leads to an unfavorable situation (core damage, containment failure, etc.), and to calculate the frequency of occurrence. PRA was established with WASH-1400 (Rasmussen, 1975) and is used widely in various countries around the world. WASH-1400 pointed out the importance of operator actions and the fact that a small break loss-of-coolant accident (LOCA) and transient events contributed to risks greater than a large break LOCA, which was evaluated in conventional deterministic safety analysis as a design-basis accident. As a result of the TMI-2 accident, the effectiveness of PRA was recognized again. In addition, because of its usefulness, it is now used actively by regulatory agencies and utilities. In Japan, PRA is used in nuclear regulatory inspections conducted by the Nuclear Regulation Authority (2019).

When the risk of an external event is evaluated using conventional PRA, one of the limitations is the difficulty in considering the timing at which nuclear power plant (NPP) structures, systems, and components (SSCs) fail. For example, phenomena such as flooding and fire affect the timing of SSC losses depending on propagation speed. Such phenomena also affect operator actions such as isolation and fire extinction. A result of conventional Level 1 flooding PRA is core damage frequency; however, this does not include core damage timing. This information is important in Level 2/3 PRA or evacuation planning.

To overcome this limitation, several studies have been conducted from a risk perspective. For example, Zheng et al. (2014) and Jang et al. (2016) analyzed the relationship between room layout and the time it took for the water level to rise in each room, and evaluated the time dependency of conditional core damage probability (CCDP) in seismic-induced internal flooding. Idaho National Laboratory conducted a detailed risk assessment by coupling computational fluid dynamics software, NEUTRINO (Sampath et al. (2016)) and thermal-hydraulic analysis using RELAP-RAVEN (Reactor Analysis and Virtual Control Environment) (Alfonsi et al. (2013) and Mandelli et al. (2015)). Jankovsky et al. (2018) analyzed the interfacing system LOCA, taking into consideration the effect of flooding due to a residual heat removal system component rupture and the time-dependent effect using ADAPT (Analysis of Dynamic Accident Progression Trees) (Hakobyan et al. (2008)). Kloos et al. (2015) performed fire PRA considering the time dependency of firefighting performance and uncertainties of parameters related to fire evolution using MCDET (Monte Carlo Dynamic Event Tree). As demonstrated in these previous studies, dynamic PRA is an effective approach that can be used to evaluate in detail the risks associated with external events. Methods and tools for dynamic PRA have been developed by many organizations; for example, ADS-IDAC

Proceedings of the 30th European Safety and Reliability Conference and the 15th Probabilistic Safety Assessment and Management Conference
Edited by Piero Baraldi, Francesco Di Maio and Enrico Zio
Published by Research Publishing, Singapore.
ISBN: 978-981-14-8593-0; doi:10.3850/978-981-14-8593-0

(Accident Dynamic Simulator coupled with the Information, Decision, and Action in a Crew context) (Diaconeasa (2018)), PyCATSHOO (PythoniC Object Oriented Hybrid Stochastic AuTomata) (Chraibi (2018)), SCAIS (Simulation Codes System for ISA) (Izquierdo (2016)), CMMC (Continuous Markov chain and Monte Carlo) (Jang (2018)), and GO-FLOW, which is a success oriented system analysis technique (Matsuoka (2014)).

The Japan Atomic Energy Agency (JAEA) has developed an integrated severe accident code, called Thermal-Hydraulic Analysis of Loss of Coolant, Emergency Core Cooling, and Severe Core Damage, version 2 (THALES2) (Kajimoto et al. (1991)), which is used particularly to measure fission product chemical behaviors (Ishikawa et al. (2017)). THALES2 was also used to evaluate the Fukushima Dai-ichi NPP accident (Ishikawa et al. (2015)). To quantify risk using simulation-based methods, the JAEA is developing a dynamic PRA tool, called Risk Assessment with Plant Interactive Dynamics (RAPID) (Zheng et al. (2018)), which enables explicit modeling of accident scenarios and occurrence probabilities.

In this study, we performed a dynamic flooding-initiated PRA of an NPP. As shown in Fig. 1, thermal-hydraulic analysis using THALES2 and flood simulations were coupled using RAPID. In the analysis, the effects of isolation and drainage were evaluated. According to the results, a distribution of core damage timing was obtained, which was difficult to treat using conventional PRA.

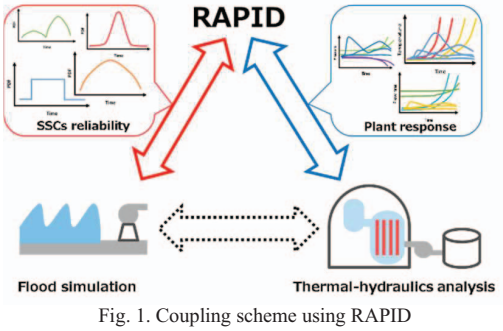

Fig. 1. Coupling scheme using RAPID

2. Method of Analysis

2.1 *Base flooding event*

The event selected for study involved internal flooding that occurred in a turbine building in a pressurized water reactor (PWR) NPP. Fig. 2 shows the turbine building compartments, and Table 1 shows the area of each section and the installed equipment. The turbine building consisted of seven sections protected by water barriers. The flood source was assumed to be a rupture in the circulating system pipes, occurring in Room1, and the leak rate was 6,000 m^3/hr based on previous research (Mitsubishi Heavy Industries, Ltd. (2006)). The layout was based on an examination of the internal flooding PRA at Kewaunee power plant (Dominion (2006)) and a report by the Nuclear Regulatory Commission (Nuclear Regulatory Commission) (2005).

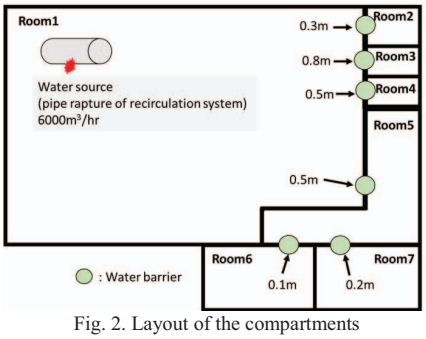

Fig. 2. Layout of the compartments

Table 1. Area of each compartment and installed equipment

Compartment	Area (m^2)	Installed equipment
Room1	4000	Alarm for flooding
Room2	100	Auxiliary Feed water pump A
Room3	50	Auxiliary Feed water pump B
Room4	80	—
Room5	600	—
Room6	300	Control panel for High Pressure Injection pump A
Room7	300	Control panel for High Pressure Injection pump B

The flooding event included various threats to SSC reliability, such as submersion, spray, water pressure, wave impact, and high-temperature steam. Wang et al. (2019) evaluated flood propagation and its impact on floating bodies in the layout of AP1000. Smith et al. (2016) performed fragility experiments and probabilistic modeling of full-scale interior doors against flood pressure. Under the conditions chosen in this research, it was assumed that the dominant failure mechanism was submergence and that this comprehensively represented the effects of flooding.

The evaluation of flood propagation was simplified using a formula based on Bernoulli's law from the viewpoint of computational cost. Specifically, only the overflow was considered as the inflow between sections. The model shown in Fig. 3 was used, and equation (1) introduced the

internal flooding PRA standard published by the Atomic Energy Society of Japan (Atomic Energy Society Japan (2012)).

$$Q_{overflow} = w \times c \times \int_0^{h_{over}} u dh_{over}$$
$$= \frac{2}{3} \times w \times c \times \sqrt{2g} \times {h_{over}}^{3/2} \quad (1)$$

$$\because \mathrm{u} = \sqrt{2gh} \quad (2)$$

Here, $Q_{overflow}$: overflow flow rate (m^3/s), w: open channel width (m), c: flow coefficient (-), u: overflow velocity (m/s), h_{over}: water level above the water barrier (m), and g : gravitational acceleration (m/s^2). The time variations in the water level in each section under this condition are shown in Fig. 4. Table 2 shows the flood propagation flow path.

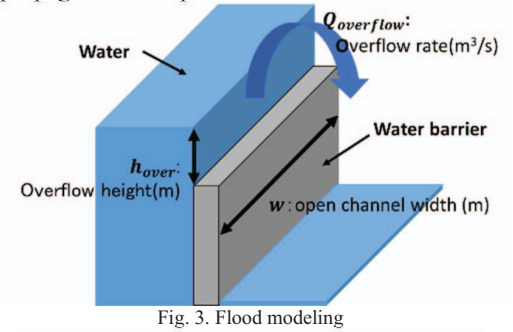

Fig. 3. Flood modeling

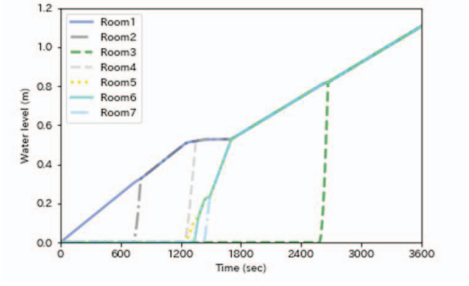

Fig. 4. Time variations in water levels in each compartment

Table 2. Flood propagation flow path

Order	Path
1	Room1 ⇒ Room2
2	Room1 ⇒ Room4
	Room1 ⇒ Room5
4	Room5 ⇒ Room6
5	Room5 ⇒ Room7
6	Room1 ⇒ Room3

2.2 *Plant model*

In this study, a simplified PWR model using THALES2 was applied in the thermal-hydraulic analysis. This model is based on a 3.4 GWt class PWR. Fig. 5 shows a schematic of the systems and Table 3 shows acronyms used in Fig. 5.

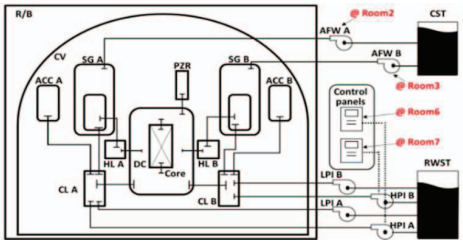

Fig. 5. PWR modeling in THALES2 (acronyms are shown in Table 3)

Table 3. Acronyms used in Fig. 5

Acronym	Full name
ACC	Accumulator injection system
AFW	Auxiliary Feed Water system
CL	Cold Leg
CST	Condensate Storage Tank
CV	Containment Vessel
DC	Down Comer
HL	Hot Leg
HPI	High Pressure Injection system
LPI	Low Pressure Injection system
PZR	Pressurizer
RWST	Refueling Water Storage Tank
R/B	Reactor Building
SG	Steam Generator

Initiated by the transient event of flooding, the incident was categorized as a high-pressure accident scenario. Therefore, the mitigation systems were a control rod drive system, an auxiliary feed water (AFW) system, a high-pressure injection (HPI) system, and power-operated relief valves. It was assumed that the equipment affected by flooding was the HPI control panels and the AFW pumps. Table 4 shows the water levels at which the respective functions were lost as a result of submergence.

Table 4. Compartments and water levels at which each mitigation system loses function

Submerged system	Compartment	Height (inch)
AFW train A	Room2	18
AFW train B	Room3	13
HPI train A	Room6	6
HPI train B	Room7	6

In this accident scenario, it was assumed that the reactor was successfully tripped at the same time as the occurrence of the flooding and that feed and breed (F&B) was successfully implemented by the operator when the alarm sounded, as long as the water level in Room1 reached 0.1 m. Then, AFW A pump lost function due to submersion, followed by the HPI control panels, and, finally, AFW B pump. Table 5 shows the timeline of plant responses in the base case. Fig. 6 shows the event tree that was used to organize the timeline shown in Table 5. The minimal cut set of core damage in this tree, MCS_{CD}, is expressed in equation (3).

$$MCS_{CD} = AFW\_A \cap HPI\_A \cap HPI\_B \cap AFW\_B \quad (3)$$

The occurrence probabilities of the components of this minimal cut set are time dependent, and their dynamic handling enables detailed evaluation.

Table 5. Timeline of base case

Time (s)	Plant response	Event symbol
0	Flooding occurrence and trip success	-
240	F&B started by alarm activation	-
1,124	AFW A pump loss of function due to submersion	AFW_A
1,393	HPI A pump loss of function due to submersion	HPI_A
1,473	HPI B pump loss of function due to submersion	HPI_B
2,635	AFW B pump loss of function due to submersion	AFW_B
18,600	Peaking cladding temperature reach 1,200 ° C	CD

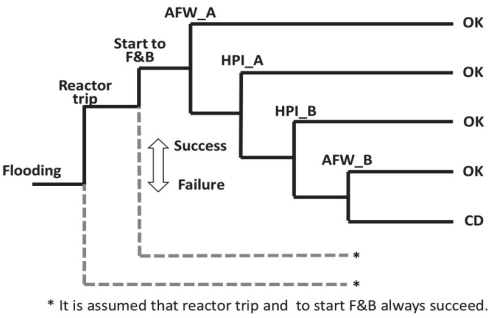

Fig. 6. Event tree

2.3 *Assumptions*

2.3.1 *Flooding source*

In the base case analysis, it was decided that the flow rate of the flood water source was 6,000 m^3/hr. However, it is difficult to estimate the parameters involved in a pipe rupture for a flooding PRA. Therefore, Fleming et al. (2004) quantified the parameters using Bayes' uncertainty analysis and developed a database. In this study, for the sake of simplicity, the probability distribution of the water flow rate was set at a normal distribution with a mean of 6,000 m^3/hr and a standard deviation of 600 m^3/hr.

2.3.2 *Failure criteria*

In a large flooding condition, the wave front ripples. Therefore, it is difficult to determine the water level uniquely in a large section. In particular, regarding flooding during a seismic event, the effects of sloshing would be expected to appear. To consider the variations in water levels, the normal distributions listed in Table 6 were set as the submergence criteria for the mitigation systems.

Table 6. Normal distributions for hypothetical submergence criteria

Submerged system	Mean (inch)	Std. (inch)
AFW train A	18	1.8
AFW train B	13	1.3
HPI train A	6	0.6
HPI train B	6	0.6

2.3.3 *Recovery actions*

- Isolation of flood source

In flooding events, isolation actions have a significant impact on event progression. Therefore, human reliability analysis (HRA) such as IDAC (Chang et al. (2007)) and Crew-module (Kloos et al. (2008)), which evaluates the reliability of operator actions, must be implemented in any detailed analysis. In this study, for the purpose of coupling the thermal-hydraulic analysis and the simple flood propagation analysis program, the following simplified HRA model was used. To simulate the timing of successful isolation, a truncated normal distribution with the following parameters was used.

The median value was the timing at which the AFW B pump was placed in Room3 and lost function (2,635 s). The standard deviation was set to 1,438 s, which was the intermediate value between the overflow alarm sounding (240 s) and

the AFW B losing function. Therefore, a truncated normal distribution with a lower limit of 240 s and an upper limit of 4,073 s was assumed (see Fig. 7 and Table 7).

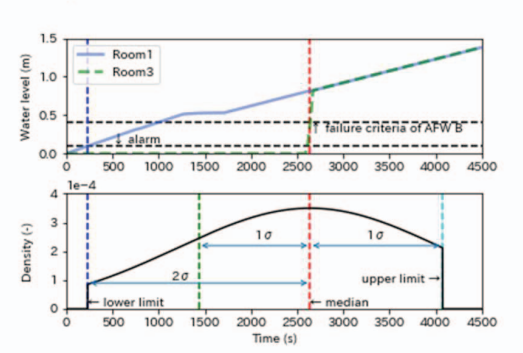

Fig. 7. Probability distribution of timing for successful isolation action

Table 7. Parameters related to the probability distribution of timing of successful isolation actions

Parameter	Setting condition (values in basic analysis)	Time (s)
Median	Submerged time of AFW pump B	2,635
Std.	Intermediate value between flooding alarm activation time and submersion time of AFW pump B	1,438
Lower limit	Flooding alarm activation time	240
Upper limit	Median +1σ	4,073

- Drainage of water

After the Fukushima Dai-ichi NPP accident, a number of utilities installed drainage pumps to prevent and mitigate flood propagation (Chubu Electric Power Co. (2011) and U.S.NRC (2018)). To reflect this safety improvement, we modeled the drainage of the flood water. The drainage pump was installed in Room1 and its drainage capacity was assumed to be 2,000 m^3/hr. This pump starts to run and drain at the same time as the flood alarm is activated.

2.3.4 *Accident analysis*

In this study, the accident scenario in THALES2 was analyzed for eight hours from the occurrence of the flooding. If peak cladding temperatures (PCTs) reached 1,200°C within this period, this was counted as a core-damaged accident sequence. For each recovery action, 10,000 cases were analyzed.

3. Results

3.1 Accident simulation without recovery

Fig. 8 shows the frequency distributions of the timing when the alarm was triggered and the equipment was submerged. The alarm timing had the lowest level of uncertainty, whereas the timing uncertainty when the AFW B lost function was the highest. This is because the sections where the inflow started late were affected notably by the rate at which the level rose as determined by the flow rate of the water source, and also by the time at which the water level in Room1 reached a constant. When evaluating flooding progress, it is necessary to consider the above points.

Fig. 9 shows the time variations in the PCTs of 10,000 cases. All cases resulted in core damage. In addition, the PCTs started to rise after approximately four hours.

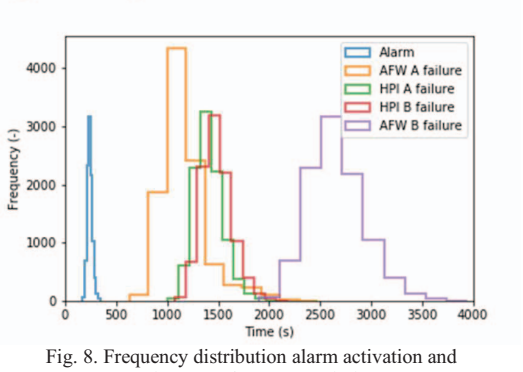

Fig. 8. Frequency distribution alarm activation and equipment submergence timing

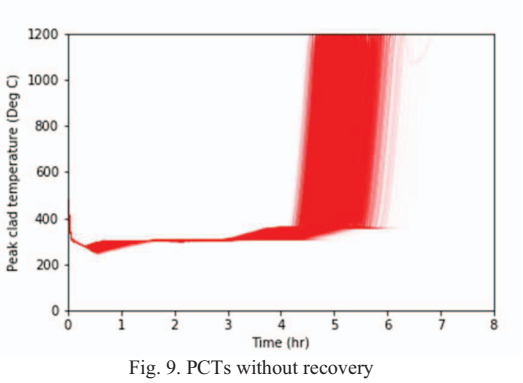

Fig. 9. PCTs without recovery

3.2 Accident simulation with isolation

Fig. 10 shows the time variations in PCTs when the isolation measure mentioned in section 2.3.3 is considered. By considering this effect, 4,550 of 10,000 cases avoided core damage. This result indicates that the effect of this action reduces CCDP by 45.5%.

There are two groups of accident sequence that do not lead to core damage: the upper sequence avoids core damage using an AFW; the lower sequence avoids core damage using F&B. Isolation leads to differences in the mitigation systems that are able to avoid loss of function, which results in these groups.

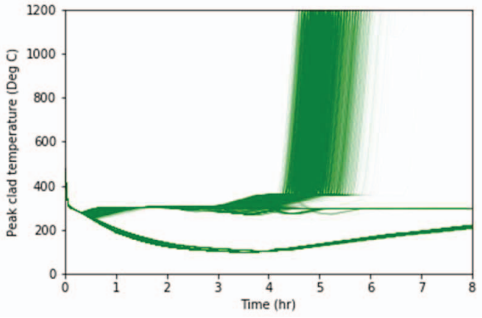

Fig. 10. PCTs with isolation

3.3 Accident simulation with drainage

Fig. 11 shows the time variations in PCTs when the drainage measure mentioned in section 2.3.3 is considered. By considering this effect, 402 of 10,000 cases avoided core damage. Drainage delayed the core damage timing. The results suggest that it becomes a more effective counter measure when combined with isolation.

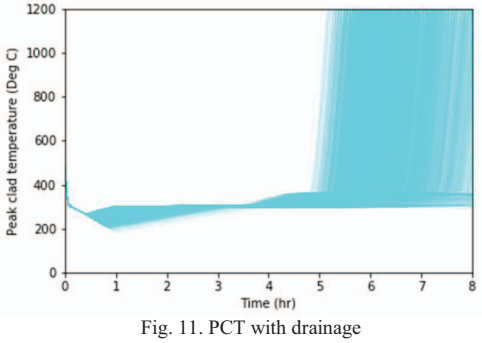

Fig. 11. PCT with drainage

3.4 Accident simulation with isolation and drainage

Fig. 12 shows the time variations in PCTs when isolation and drainage measures are considered. Under this condition, 8,743 of 10,000 cases avoided core damage. The results suggest that combining isolation and drainage is the most effective method of flood mitigation.

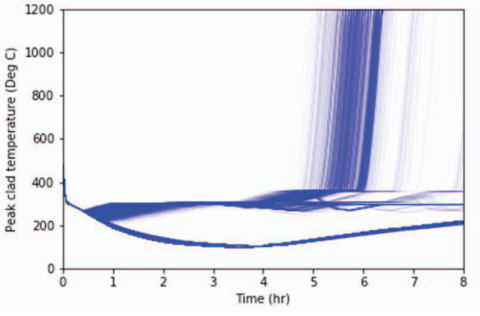

Fig. 12. PCTs with isolation and drainage

3.5 Comparison of recovery effects

Fig. 13 shows the frequency distributions of core damage timing for all conditions. By comparing the results shown by the red line (without recovery) and those shown by the green line (with isolation), it can be seen that the frequency of late core damage is reduced when the isolation measure is considered. This is because loss of function due to submergence occurs at a later time. This effect is caused by the relationship between the flood flow rate and the timing of the successful isolation action. As mentioned in section 2.3.3, it is considered necessary to apply an advanced HRA method in order to conduct a detailed evaluation.

By comparing the results shown by the red line (without recovery) and those shown by the cyan line (with drainage), it can be seen that the timing of the occurrence of core damage is delayed by drainage. This is because the speed at which the water level rises is reduced by drainage, and, therefore, the occurrence of submergence is delayed.

The results show that core damage can be avoided most effectively by combining isolation and drainage (blue line). Table 8 shows the statistical parameters of these distributions.

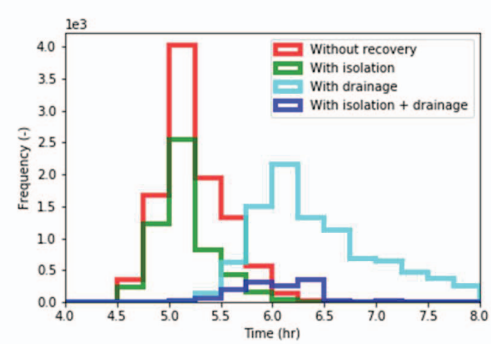

Fig. 13. Frequency distributions of core damage timing

Table 8. Statistical parameters of core damage timing

Recovery	Mean (hr)	Median (hr)	Std. (hr)
Ignore	5.22	5.17	0.31
Isolation only	5.13	5.11	0.28
Drainage only	6.47	6.28	0.65
Isolation and drainage	6.02	6.00	0.48

4. Conclusions

In this study, thermal-hydraulic simulations were coupled with flood propagation analyses using the RAPID framework, and the temporal distributions of core damage occurrences were evaluated. These distributions provide useful information because they cannot be obtained by conventional Level 1 PRA and are important inputs for Level 2/3 PRA.

In addition, a simple model was used to evaluate the isolation of flood water sources by operator actions and drainage using a pump. Although hypothetical assumptions affected the simulation results, the effects of the recovery actions were evaluated more realistically using this method.

As a result, this study demonstrated how THALES2-RAPID can be used for dynamic PRA, considering the timing of the loss of safety systems due to flooding.

The following items are suggested as areas for future work based on this study.

- Application of a detailed HRA method

In this study, the isolation action was modeled simply using probability distribution based on equipment failure timings. As a result, the effect of the isolation could be quantitatively evaluated. For a more detailed evaluation, it is necessary to understand the effectiveness of the isolation using the HRA method. At the same time, it is necessary to obtain information on environmental degradation due to flooding, such as access routes.

- Evaluation using more detailed simulation

The simple formula used in this study is a rational calculation based on Bernoulli's law; however, when considering the actual phenomena, a number of threats to the reliability of SSCs are described in section 2.1. In order to understand these effects, it is necessary to obtain detailed information on plant sections and equipment locations, as in previous studies, and to perform fluid analysis using particle methods etc.

Acknowledgments

The development of RAPID is supported financially by the Nuclear Regulation Authority, Japan. We are also grateful to Mr. Jojima, Mr. Idei, Mr. Fujiwara, and Mr. Watanabe of the Nuclear Regulation Authority, Japan, for the useful discussions.

References

Alfonsi, A., C. Rabiti, D. Mandelli, J. Cogliati and R. Kinoshita (2013). Raven as a tool for dynamic probabilistic risk assessment: Software overview. *In proceedings of International Conference on Mathematics and Computational Methods Applied to Nuclear Science and Engineering (M&C2013)*.

Atomic Energy Society Japan (2012). Implementation Standard Concerning the Internal Flooding Probabilistic Risk Assessment of Nuclear Power Plants: 2012, *AESJ-SC-RK005: 2012*. [in Japanese]

Chang, Y and A. Mosleh (2007) Cognitive modeling and dynamic probabilistic simulation of operating crew response to complex system accidents. Part 1: Overview of the IDAC model*, 92,* 997-1013.

Chubu Electric Power Co. (2011). Tsunami Countermeasures at Hamaoka Nuclear Power Station.

Chraibi, H. D. Vasseur, Le Duy TD and M. Hassanaly (2018). Addressing Critical Dependencies in the Probabilistic Performance Assessments of Multi-Purpose Systems with PyCATSHOO. *In proceedings of 14th International Conference on Probabilistic Safety Assessment and Management (PSAM14)*.

Diaconeasa, M. and A. Mosleh (2018). Discrete Dynamic Event Tree Uncertainty Quantification in the ADS-IDAC Dynamic PSA Software Platform. *In proceedings of 14th International Conference on Probabilistic Safety Assessment and Management (PSAM14)*.

Dominion (2006). Internal Flooding Risk Reduction Activities.

Fleming, K. and B. Lydell (2004). Database development and uncertainty treatment for estimating pipe failure rates and rupture frequencies. *Reliability Engineering and System Safety, 86*, 227-246.

Hakobyan, A., T. Aldermir, R. Denning, S. Dunagan, D. Kunsman, B. Rutt and U. Catalyurek (2008). Dynamic feneration of accident progression event trees. *Nuclear Engineering and Design, 238,* 3457-3467.

Ishikawa, J., K. Kawaguchi and Y. Maruyama (2015). Analysis for iodine release from unit 3 of Fukushima Dai-ichi nuclear power plant with consideration of water phase iodine chemistry. *Journal of Nuclear Science and Technology, 52,* 308-314.

Ishikawa, J., T. Sugiyama and Y. Maruyama (2017). Source Term Analysis Considering

B4C/Steel Interaction and Oxidation During Severe Accidents. *In proceedings of 25th International Conference on Nuclear Engineering (ICONE-25)*.

Izuquirdo, J., J. Hortal, M. Sanchez, E. Melendez, C. Queral and J. Ricas-Lewicky (2016). Current Status and Applications of ISA (Integrated Safety Assessment) and SCAIS (Simulation Code System for ISA). *in proceedings of 13th International Conference on Probabilistic Safety Assessment and Management (PSAM13)*.

Jang, S. and A. Yamaguchi (2018). Dynamic scenario quantification for level 2 PRA of sodium-cooled fast reactor based on continuous Markov chain and Monte Carlo method coupled with meta-model of thermal-hydraulic analysis. *Journal of Nuclear Science and Technology, 55*, 850-858.

Jang, S., T. Suzuki, and A. Yamaguchi (2016). Dynamic Level 1 PRA of Seismic-induced Internal Flooding in Nuclear Power Plant. *in proceedings of 13th International Conference on Probabilistic Safety Assessment and Management (PSAM13)*.

Jankovsky, Z., M. Denman and T. Aldemir (2018). A Dynamic Coupled-Code Assessment of Mitigation Actions in an Interfacing System Loss of Coolant Accident. *In proceedings of 14th International Conference on Probabilistic Safety Assessment and Management (PSAM14)*.

Kajimoto, M., K. Muramatsu, N. Watanabe, M. Funasako, and T. Noguchi (1991). Development of THALES-2: a computer code for coupled thermal-hydraulics and fission product transport analyses for severe accident at LWRs and its application to analysis of fission product revaporization phenomena. *In proceedings of International Topical Meeting on Safety of Thermal Reactors*.

Kloos, M. and J. Pescheke (2008). Consideration of human actions in combination with the probabilistic dynamics method Monte Carlo dynamic event tree. *Journal of Risk and Reliability, 222,* 303-313.

Kloos, M. and J. Pescheke (2015). Improved Modelling and Assessment of the Performance of Firefighting Means in the Frame of a Fire PSA. *Science and Technology of Nuclear Installations, 2015*.

Mandelli, D., S. Prescott, C. Smith, A. Alfonsi, C. Rabiti, J.Cogliati and R. Kinoshita (2015). Modeling of a Flooding Induced Station Blackout for a Pressurized Water Reactor Using the RISMIC Toolkit. *In proceedings of International Topical Meeting on Probabilistic Safety Assessment and Analysis (PSA2015)*.

Matsuoka, T. (2014). Estimation of dynamic behavior of nuclear power plant system state under severe accident conditions. *Nuclear Safety and Simulation, 5,* 197-204.

Mitsubishi Heavy Industries, Ltd. (2006). A survey on internal flood problem of PWR. [in Japanese]

Nuclear Regulation Authority, Japan (2019). Convention on Nuclear Safety National Report of Japan for 8th Review Meeting.

Nuclear Regulatory Commission Inspection report 05000305/2005011 (DRP) (2005). PRELIMINARY GREATER THAN GREEN FINDING KEWAUNEE POWER STATION.

Rasmussen, N. (1975). Reactor safety study: An assessment of accident risks in U.S. commercial nuclear power plants. *NUREG-75/014, WASH-1400*.

Sampath, R., N. Montanari, N. Akinci, S. Prescott and C. Smith (2016). Large-scale solitary wave simulation with implicit incompressible SPH. *Journal of Ocean Engineering and Marine Energy, 2,* 313-329.

Smith, C., B. Bhandari, C. Muchmore, A. Tahhan, A. Wells, L. Nichols and C. Pope (2016). Flooding Fragility Experiments and Prediction. *INL/EXT-16-39963*.

U. S. NRC (2018). Safety Enhancements after Fukushima.

Wang, Z., F. Hu, G. Duan, K. Shibata and S. Koshizuka (2019). Numerical modeling of floating bodies transport for flooding analysis in nuclear reactor building. *Nuclear Engineering and Design, 341,* 390-405.

Zheng, X., A. Yamaguchi, and T. Takata (2014). Quantitative common cause failure modeling for auxiliary feedwater system involving the seismic-induced degradation of flood barriers. *Journal of Nuclear Science and Technology, 51*, 332-342.

Zheng, X., H. Tamaki, T. Sugiyama and Y. Maruyama (2018). Severe Accident Scenario Uncertainty Analysis using the Dynamic Event Tree Method. *In proceedings of 14th International Conference on Probabilistic Safety Assessment and Management (PSAM14)*.